


High-harmonic generation in GaAs beyond the perturbative regimePeiyu Xia¹,^{*}† Tomohiro Tamaya¹,^{*}‡ Changsu Kim, Faming Lu, Teruto Kanai, Nobuhisa Ishii¹,
Jiro Itatani¹, Hidefumi Akiyama, and Takeo Kato*The Institute for Solid State Physics, The University of Tokyo, Kashiwa 277-8581, Japan* (Received 10 April 2020; revised 21 May 2021; accepted 2 September 2021; published 27 September 2021)

The field-intensity dependence of high-harmonic generation in bulk gallium arsenide is studied. We experimentally find the oscillatory behavior at high fields where a perturbative scaling law no longer holds. By constructing a theoretical framework based on the Luttinger-Kohn model, we succeed in reproducing the observed oscillatory behavior. The qualitative agreement between the experiment and theory indicates that field-induced dynamic band modification is crucial in the nonperturbative regime. We show that the oscillatory behavior is naturally understood by dynamic localization that is based on the Floquet subband picture.

DOI: [10.1103/PhysRevB.104.L121202](https://doi.org/10.1103/PhysRevB.104.L121202)

The nonperturbative properties of high-harmonic generation (HHG) in gaseous media, such as plateau and cutoff structures, originate from subcycle electron dynamics and can be used to produce short-wavelength attosecond pulses [1–6]. Moreover, in the past decade, HHG has been experimentally observed in solids; these studies have ushered in an era of high-field condensed-matter science [7–12]. In contrast to gaseous media, solids have the vastly diverse nature such as in their band structures, energy gaps, crystalline anisotropy, and magnetism. It has thus far been experimentally and theoretically investigated in various solids [13–28], but comprehensive understanding of the crossover behavior from the perturbative to the nonperturbative regime has not been gained yet. Such an understanding requires a unified viewpoint connecting the perturbative to nonperturbative regimes. This study will provide a way toward a novel optical technology.

In the perturbative regime, it is known that the intensity of the n th-order harmonics obeys an E^{2n} scaling law with respect to the field amplitude E [29–31]. In the conventional formulation of nonlinear optics using the Bloch basis, this scaling law is successfully explained by the multiphoton interband transition of Bloch electrons. The E^{2n} scaling, however, breaks down at sufficiently high fields (typically at several MV/cm). In recent theoretical studies, this nonperturbative nature of HHG is explained by the alternative formulation, in which intraband electron acceleration motion is taken into account with a new basis called the Houston basis [32–36]. In spite of these theoretical developments, it has not been clarified yet how the properties of HHG in the nonperturbative regime are seamlessly connected to those in the perturbative regime where the E^{2n} scaling holds. For a clear understanding of this crossover behavior, accurate measurement of the field-intensity dependencies of HHG is crucial and indispensable.

In addition, it is highly required to attempt theoretical description in one formulation and to verify its correctness by making a precise comparison between the theoretical predictions and the experimental data.

Bulk gallium arsenide (GaAs) has been intensively studied in the field of nonlinear optical physics and for applications [37–47] because of its direct band gap, high electron mobility, and high purity that can suppress relaxation processes. Recently, the employment of reflection geometry has become the key to avoiding propagation effects such as phase mismatch in HHG in bulk materials [25,48,49]. In addition, GaAs can be regarded as a representative semiconductor in a sense that its qualitative features are expected to be observed also in other semiconductors. It can be described naturally by a general theoretical framework which was developed for semiconductors [50–59]. Thus, GaAs is an ideal platform for exploring HHG in solids from the perturbative to nonperturbative regime.

In this letter, we experimentally and theoretically investigate the field-intensity dependence of HHG in GaAs. The experimental result shows the perturbative scaling law at the weak-field regime and the oscillatory behavior at the high-field regime. To explain this feature, we establish a theoretical framework by extending the conventional Luttinger-Kohn model using the formulation with the Bloch basis. By performing the numerical calculation, we find that the oscillatory behavior reflects the field-induced time-dependent band structure. The unified picture connecting from the perturbative to nonperturbative regime obtained in this paper would provide reasonable interpretation of the HHG mechanism.

The experiments were carried out by using an intense mid-infrared (MIR) laser irradiating a GaAs sample, as shown in Fig. 1(a). A two-stage KTiOAsO₄ (KTA)-based optical parametric amplifier with single-plate compression [60] using an antireflection-coated 5-mm-thick Ge window generated linearly polarized 80-fs pulses at 3.65 μm , which corresponds to a photon energy of 0.34 eV. These MIR pulses were focused on the (110) surface of a 400- μm -thick GaAs sample at room temperature and at an incidence angle of 5 deg. We took advantage of the reflection geometry to avoid propagation

*These authors contributed equally to this work.

†Corresponding author: xia@issp.u-tokyo.ac.jp‡Corresponding author: tamaya@issp.u-tokyo.ac.jp

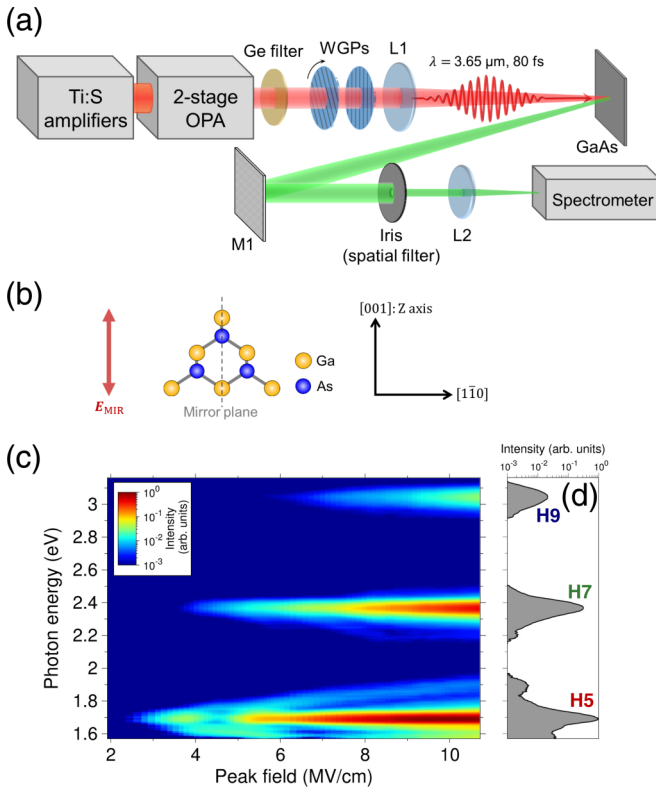


FIG. 1. (a) Experimental setup for HHG in reflection geometry using bulk GaAs and MIR laser source. Ti:sapphire regenerative and multipass amplifiers (450 Hz, 5 mJ, 70 fs) were used to pump the optical parametric amplifier (OPA) [60]. WGPs, a pair of wire-grid polarizers; L1 ($f = 300$ mm) and L2 ($f = 50$ mm), CaF₂ lenses; M1 ($R = 100$ mm), Al-coated concave mirror. (b) Structure of the (110) surface of GaAs and direction of the laser polarization. (c) Field-intensity dependencies of the fifth, seventh, and ninth harmonic spectra. (d) HHG spectrum at the peak field of 10 MV/cm.

effects in the HHG process. A pair of wire-grid polarizers were used to adjust the laser-field intensity while keeping the linear polarization along the [001] axis. The peak field was estimated to be up to 12 MV/cm inside the sample, without damage. The HHG spectra were detected using a fiber-coupled spectrometer (QEPro, Ocean Optics), which showed only odd-order harmonics due to the inversion symmetry of GaAs [Fig. 1(b)].

We measured the HHG intensities integrated around each of the harmonic spectral peaks as a function of the peak field of the MIR pulses from 2 to 12 MV/cm. The measured field-intensity dependencies were found to vary with the transverse position of the diverging HHG beam (for details, see the Supplemental Material Sec. IV [61]) that was probably caused by the transverse intensity distribution of the MIR beam, as in an experiment in gaseous media [62]. To avoid spatial averaging of the field-intensity dependencies, we inserted an iris in the center of the high harmonic beam. This spatial filtering allowed us to observe the fine-scale oscillatory behavior more clearly [Fig. 2(a)]. It also helped to minimize the signal level of background fluorescence around the band gap (1.42 eV) of GaAs. In regard to the HHG spectra shown in Figs. 1(c) and 1(d), the observed harmonics often had different spectral

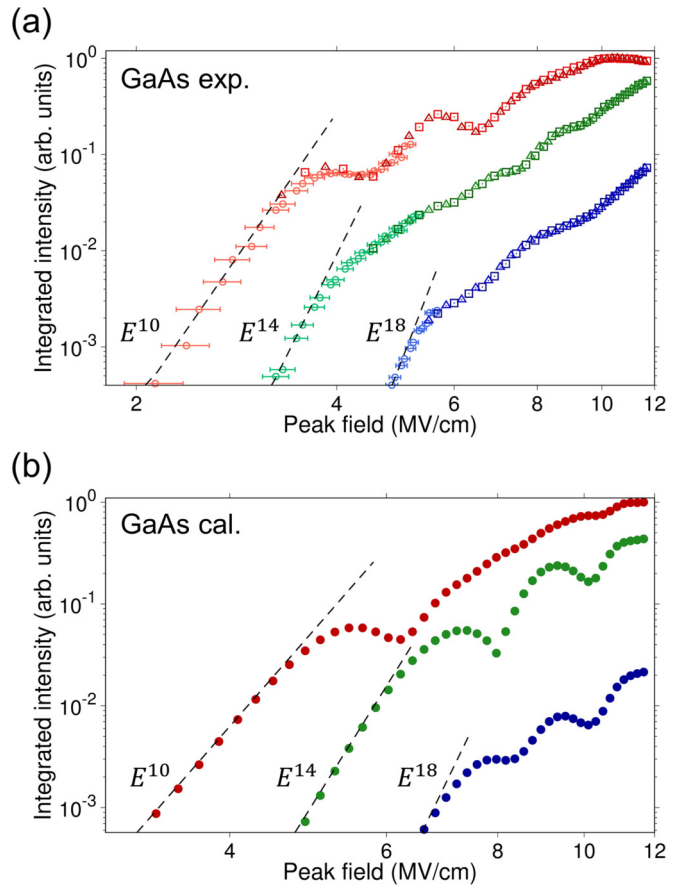


FIG. 2. (a) Field-intensity dependencies of the fifth (red), seventh (green), and ninth (blue) HHG intensities. Two data sets (squares and triangles) were measured in a single sweep starting from 2 to 12 MV/cm and then from 12 to 2 MV/cm, respectively. Small HHG signals (circles) were measured with a longer acquisition time. (b) Calculated results of the Luttinger-Kohn model. In the weak-field regime, the harmonic intensities almost obey an E^{2n} perturbative scaling law for both the measured and calculated results (dashed black lines).

shapes, part of which was modulated with increasing field intensity.

Figure 2(a) shows that the intensities of the fifth, seventh, and ninth harmonics did not saturate monotonically with increasing the laser intensity, but rather exhibited oscillatory behaviors. As the field intensity was increased, the oscillatory behaviors appeared above 4, 5, and 6 MV/cm for the fifth, seventh, and ninth harmonics, respectively, where they started to deviate from the perturbative scaling law. The oscillation peaks appeared well beyond the perturbative regime, and their positions varied with the harmonic order. Two consecutive measurements reproduced the intensities and the oscillatory behaviors, indicating no irreversible changes in the sample after each laser irradiation. An explanation of these experimental results will require clarification of the crossover of HHG from the perturbative to the nonperturbative regime as well as the physical origin of the oscillatory behavior.

To analyze these experimental results, we employed an eight-band Luttinger-Kohn model, which includes conduction, heavy-hole, light-hole, and split-off bands for both

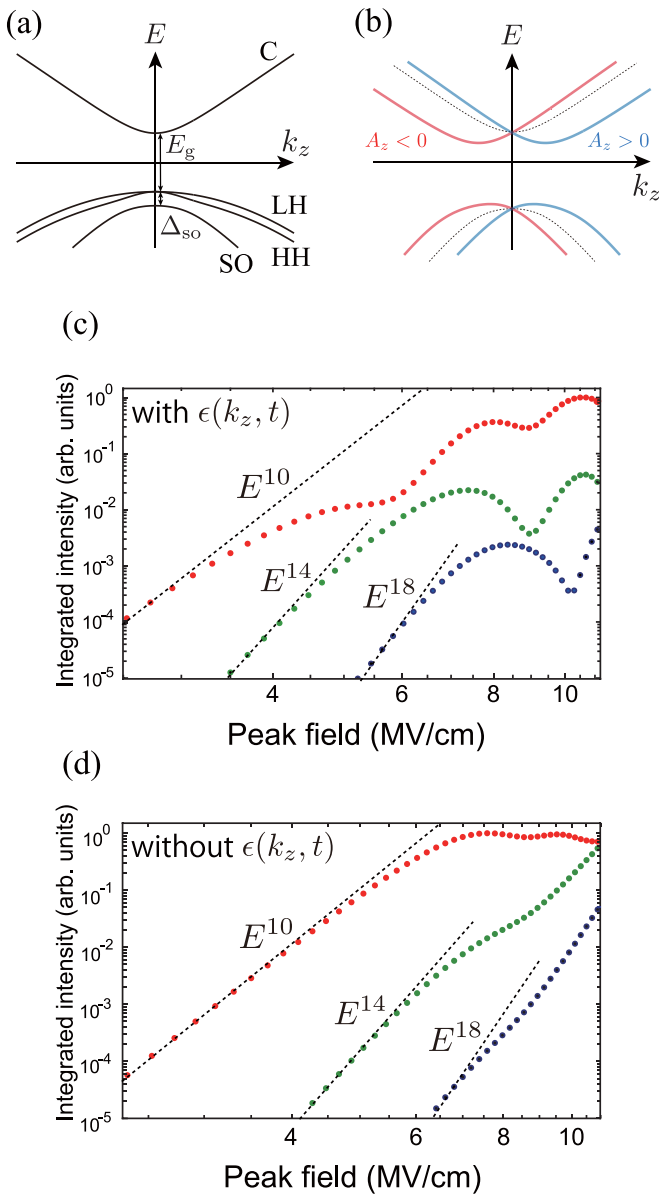


FIG. 3. (a) Schematic diagram of the band structure of GaAs in the absence of an external field for $\mathbf{k} = (0, 0, k_z)$. The four bands, each of which is twofold degenerate, correspond to conduction (C), light-hole (LH), heavy-hole (HH), and split-off (SO) bands. We express the band gap and split-off band energy as E_g and Δ_{SO} . (b) Schematic diagram of the dispersion relations of the simplified model (the Kane model) under an external field. The blue and red lines indicate dispersion relations for $A_z > 0$ and $A_z < 0$. Numerical results of field-intensity dependence of fifth (red dots), seventh (green dots), and ninth (blue dots) harmonics in GaAs based on the Kane model with (c) and without (d) the band modification term $\epsilon(k_z, t)$. These results indicate the effect of the field-induced dynamic band modification on the oscillatory behavior.

spin-up and spin-down components [see Fig. 3(a)]. Here we briefly describe the model (the details are in the Supplemental Material [61]). The model Hamiltonian is written in the form

$$H_0 = \sum_{k\sigma\sigma'} \sum_{l,l'} c_{kl\sigma'}^\dagger (H_k)_{l\sigma,l'\sigma'} c_{kl'l'\sigma'}, \quad (1)$$

where $c_{kl\sigma}$ is the annihilation operator of electrons for the Bloch states constructed from the atomic states of an orbital l ($= s, p_x, p_y, p_z$) and a spin σ . The matrix element $(H^k)_{l\sigma,l'\sigma'}$ is explicitly given in the Supplemental Material [61]. We describe the external field by the vector potential $\mathbf{A}(t) = (0, 0, A_z(t))$. The Hamiltonian for the light-matter interaction is then written as [63]

$$H_I = \sum_{k\sigma} (-i\hbar\Omega_R(t) c_{k\sigma}^\dagger c_{k p_z \sigma} + \text{H.c.}). \quad (2)$$

Here $\Omega_R(t) = (e/c\hbar^2)A_z(t)P_0$ is the Rabi frequency [64], and P_0 is the dipole matrix element [65]. Neglecting the dephasing effect, the system can be regarded as a collection of quantum eight-state wave functions, which are defined at each wave number \mathbf{k} . We calculated the time evolution of the quantum state under an external field by solving the time-dependent Schrödinger equation for each wave number with the initial condition that all three valence bands are occupied by electrons. Note that the quantum dynamics of the time-dependent Hamiltonian induces nonadiabatic excitation through the Landau-Zener transition [66]. The HHG spectrum was obtained by Fourier transformation of the current induced by the external field.

Figure 2(b) shows the numerical results of the HHG intensities in GaAs as a function of the field intensity. Here the red, green, and blue dots indicate the fifth, seventh, and ninth harmonics, respectively. This figure shows that the intensities of the n th-order harmonics follow the scaling law of perturbative nonlinear optics $I_n \propto E^{2n}$ for the weak field, while they start to show oscillatory behavior in the nonperturbative regime. These behaviors are consistent with the experimental results [Fig. 2(a)], although the numerical results somewhat emphasize the dips. We presume that this difference may come from the spatial variation of the field amplitude due to incomplete spatial filtering in the experiment and dephasing effects due to carrier-carrier scattering which are not considered in the present calculation.

To understand the origin of the oscillatory behavior in Fig. 2, let us introduce a simplified model (the Kane model) derived from the Luttinger-Kohn model [65,67] by restricting the bands to the conduction and split-off bands (see the Supplemental Material Sec. II [61]). Neglecting the spin-flip process and abbreviating the spin index, the Hamiltonian of the Kane model reduces to a 2×2 matrix of the form

$$H_k^{\text{eff}} = \begin{pmatrix} E_c(\mathbf{k}) - 2\epsilon(k_z, t) & -\hbar\Omega_R(t)/\sqrt{3} \\ -\hbar\Omega_R(t)/\sqrt{3} & E_v(\mathbf{k}) + 2\epsilon(k_z, t)/3 \end{pmatrix}, \quad (3)$$

where $E_c(\mathbf{k})$ and $E_v(\mathbf{k})$ are the dispersion of the conduction and valence bands, respectively, and $\epsilon(k_z, t) = (P_0 k_z / E_g) \Omega_R(t)$ is the term that changes the band dispersion [21,66,68,69]. Hereafter we call the change of the band structure due to $\epsilon(k_z, t)$ “band modification” [70]. Now, the diagonal element of H_k^{eff} represents the band dispersion of the conduction and valence bands modified by the external field $\Omega_R(t)$ [$\propto A_z(t)$] [see Fig. 3(b)]. The effect of this band modification includes a concept of intraband acceleration; the standing Bloch electron under the dynamically modified band structure is equivalent to electrons accelerated by the external electric field in a fixed band structure [21,66,68].

We should take care that this band modification does not agree to the conventional acceleration theorem wherein \mathbf{k} is simply replaced by $\mathbf{k} - (e/c)\mathbf{A}(t)$ [see Eq. (3)], since it also causes the reduction in the band-gap energy (dynamical Franz-Keldysh effect). The HHG intensities calculated for this model qualitatively reproduce the oscillatory structure, as shown in Fig. 3(c). This result indicates that the number of valence bands is not essential to the appearance of the oscillation. We calculate the HHG intensities for an artificial Hamiltonian obtained by omitting $\epsilon(k_z, t)$ to consider pure interband transitions by the off-diagonal element of H_k^{eff} . As a result, the dips become less prominent as shown in Fig. 3(d). Therefore, the temporal change in the band dispersions represented by $\epsilon(k_z, t)$ is important compared to the interband transitions to the appearance of the oscillatory behavior.

Let us discuss the physical origin of the oscillatory behavior. For a continuous wave described by $\Omega_R(t) = \Omega_{R0} \cos \omega t$ (ω : the frequency of the incident light), the energy levels at each wave number are split into Floquet subbands [69] due to the band modification term $\epsilon(k_z, t)$ [21,66,68]. Then, a matrix element for interband transition accompanying n -photon absorption/emission is renormalized, and is multiplied with the n th-order Bessel function $J_n(A_{c,v}/\omega)$ where $A_c = 3A_v = 2P_0k_z\Omega_{R0}/E_g$ [71]. We note that this Bessel function becomes zero at specific values of $A_{c,v}/\omega$. This consideration indicates that the oscillatory behavior of the high harmonics reflects suppression of the effective transition probability at specific values of $A_{c,v}/\omega$, which is called dynamical localization or destruction of tunneling [72–75]. Note that the positions of the dips are influenced by various external conditions, such as the wavelength or the chirp of the incident electric field. This indicates that transient population dynamics caused by electronic excitation on a subcycle timescale also affects the field-intensity dependence of HHG.

In the framework of perturbative nonlinear optics, the excitation processes are described by multiphoton absorption in a fixed band structure or a virtual level, and their transition probabilities become a monotonic function of the field intensity that leads to the $I_n \propto E^{2n}$ scaling law [29–31]. In the strong electric field, however, temporal modification of the band structures becomes significant [21,66,68,69], and the excitation probability is expected to show nonmonotonic behavior as a function of the field intensity. Actually, recent HHG experiments on ZnSe, sapphire, and Si have observed similar oscillatory behavior for the tenth (2.4 eV), seventh (11 eV), and seventh (3.9 eV) harmonics, respectively [18,22,25], all of which were close to the direct-band-gap energies of the corresponding materials. Parts of them were fitted by a power

function [22] or by modeling HHG induced by the intraband current in which electrons and holes are accelerated according to Bloch's theorem [18]. Although these analyses were in good agreement with the observed HHG signals, the fine-scale oscillatory behavior was not reproduced. In contrast, our work provides clear evidence that above-band-gap HHG in GaAs exhibits oscillations in both experiment and theory. Therefore, our clarification of its physical origin, i.e., the field-induced dynamic band structure, will be essential to gaining a full understanding of extreme nonlinear optics in solids. In addition, our findings could be connected to HHG in the gas phase [62,76–78] and other high-field phenomena including dynamical localization or destruction of tunneling [72–75], which also shows oscillatory behavior as a function of the field intensity.

In conclusion, we experimentally investigated HHG in GaAs by using reflection geometry and spatial filtering to avoid propagation effects and spatial averaging. We found that the intensities of the observed high harmonics did not monotonically saturate but rather exhibited oscillatory behavior with increasing field intensity. By constructing a theoretical framework using the Luttinger-Kohn model, we succeeded in qualitatively reproducing this oscillatory behavior. By analyzing a simplified theory derived from the Luttinger-Kohn model (the Kane model), we showed that this oscillatory behavior originates from the field-induced dynamic band modulation due to the diagonal elements of the time-dependent light-matter interaction matrix. The oscillatory behavior was related to the Floquet subband picture with the transition amplitude expressed in terms of Bessel functions [69], whose behavior leads to dynamical localization. We note that the present interpretation is based on the Bloch basis. One may ask what kind of a physical picture should be provided by the alternative formulation using the Houston basis [32,35,36]. This question is left as a future problem. The findings of this letter give a foundation for understanding the crossover of HHG from the perturbative to nonperturbative regime and opens up the possibility of novel optical technologies, such as strong-field coherent control of solid HHG and Floquet engineering of dressed states in solids.

The authors acknowledge support from the Japan Society for the Promotion of Science (JSPS KAKENHI Grants No. JP18H01469, No. JP18H05250, No. JP19H02623, No. JP19K14624, and No. JP20K03831). H.A. also acknowledges support by the MEXT Quantum Leap Flagship Program (MEXT Q-LEAP). P.X. was supported by the Advanced Leading Graduate Course for Photon Science (ALPS).

[1] P. B. Corkum, *Phys. Rev. Lett.* **71**, 1994 (1993).
 [2] M. Protopapas, C. H. Keitel, and P. L. Knight, *Rep. Prog. Phys.* **60**, 389 (1997).
 [3] T. Brabec and F. Krausz, *Rev. Mod. Phys.* **72**, 545 (2000).
 [4] P. Agostini and L. F. DiMauro, *Rep. Prog. Phys.* **67**, 813 (2004).
 [5] P. B. Corkum and F. Krausz, *Nat. Phys.* **3**, 381 (2007).
 [6] F. Krausz and M. Ivanov, *Rev. Mod. Phys.* **81**, 163 (2009).
 [7] S. Ghimire, A. D. DiChiara, E. Sistrunk, P. Agostini, L. F. DiMauro, and D. A. Reis, *Nat. Phys.* **7**, 138 (2011).

[8] O. Schubert, M. Hohenleutner, F. Langer, B. Urbanek, C. Lange, U. Huttner, D. Golde, T. Meier, M. Kira, S. W. Koch, and R. Huber, *Nat. Photon.* **8**, 119 (2014).
 [9] T. T. Luu, M. Garg, S. Y. Kruchinin, A. Moulet, M. T. Hassan, and E. Goulielmakis, *Nature (London)* **521**, 498 (2015).
 [10] M. Hohenleutner, F. Langer, O. Schubert, M. Knorr, U. Huttner, S. Koch, M. Kira, and R. Huber, *Nature (London)* **523**, 572 (2015).

- [11] G. Vampa, T. J. Hammond, N. Thiré, B. E. Schmidt, F. Légaré, C. R. McDonald, T. Brabec, and P. B. Corkum, *Nature (London)* **522**, 462 (2015).
- [12] S. Ghimire and D. A. Reis, *Nat. Phys.* **15**, 10 (2019).
- [13] L. Plaja and L. Roso-Franco, *Phys. Rev. B* **45**, 8334 (1992).
- [14] K. A. Pronin, A. D. Bandrauk, and A. A. Ovchinnikov, *Phys. Rev. B* **50**, 3473 (1994).
- [15] D. von der Linde, T. Engers, G. Jenke, P. Agostini, G. Grillon, E. Nibbering, A. Mysyrowicz, and A. Antonetti, *Phys. Rev. A* **52**, R25 (1995).
- [16] F. H. M. Faisal and J. Z. Kamiński, *Phys. Rev. A* **56**, 748 (1997).
- [17] G. Ndashimiye, S. Ghimire, M. Wu, D. A. Browne, K. J. Schafer, M. B. Gaarde, and D. A. Reis, *Nature (London)* **534**, 520 (2016).
- [18] A. A. Lanin, E. A. Stepanov, A. B. Fedotov, and A. M. Zheltikov, *Optica* **4**, 516 (2017).
- [19] H. Liu, Y. Li, Y. S. You, S. Ghimire, T. F. Heinz, and D. A. Reis, *Nat. Phys.* **13**, 262 (2017).
- [20] Y. S. You, D. A. Reis, and S. Ghimire, *Nat. Phys.* **13**, 345 (2017).
- [21] N. Yoshikawa, T. Tamaya, and K. Tanaka, *Science* **356**, 736 (2017).
- [22] H. Kim, S. Han, Y. W. Kim, S. Kim, and S.-W. Kim, *ACS Photon.* **4**, 1627 (2017).
- [23] S. Jiang, J. Chen, H. Wei, C. Yu, R. Lu, and C. D. Lin, *Phys. Rev. Lett.* **120**, 253201 (2018).
- [24] F. Langer, C. Schmid, S. Schlauderer, M. Gmitra, J. Fabian, P. Nagler, C. Schüller, T. Korn, P. Hawkins, J. Steiner, U. Huttner, S. Koch, M. Kira, and R. Huber, *Nature (London)* **557**, 76 (2018).
- [25] G. Vampa, Y. S. You, H. Liu, S. Ghimire, and D. A. Reis, *Opt. Express* **26**, 12210 (2018).
- [26] R. E. F. Silva, I. V. Blinov, A. N. Rubtsov, O. Smirnova, and M. Ivanov, *Nat. Photon.* **12**, 266 (2018).
- [27] H. Hirori, P. Xia, Y. Shinohara, T. Otobe, Y. Sanari, H. Tahara, N. Ishii, J. Itatani, K. L. Ishikawa, T. Aharen, M. Ozaki, A. Wakamiya, and Y. Kanemitsu, *APL Mater.* **7**, 041107 (2019).
- [28] B. Cheng, N. Kanda, T. N. Ikeda, T. Matsuda, P. Xia, T. Schumann, S. Stemmer, J. Itatani, N. P. Armitage, and R. Matsunaga, *Phys. Rev. Lett.* **124**, 117402 (2020).
- [29] A. Yariv and P. Yeh, *Optical Waves in Crystals* (Wiley, New York, 1984).
- [30] Y. R. Shen, *The Principles of Nonlinear Optics* (Wiley, New York, 1984).
- [31] R. W. Boyd, *Nonlinear Optics* (Academic Press, San Diego, 1992).
- [32] P. G. Hawkins, M. Y. Ivanov, and V. S. Yakovlev, *Phys. Rev. A* **91**, 013405 (2015).
- [33] G. Vampa, C. R. McDonald, G. Orlando, D. D. Klug, P. B. Corkum, and T. Brabec, *Phys. Rev. Lett.* **113**, 073901 (2014).
- [34] D. Golde, T. Meier, and S. W. Koch, *Phys. Rev. B* **77**, 075330 (2008).
- [35] M. Wu, S. Ghimire, D. A. Reis, K. J. Schafer, and M. B. Gaarde, *Phys. Rev. A* **91**, 043839 (2015).
- [36] C. R. McDonald, G. Vampa, P. B. Corkum, and T. Brabec, *Phys. Rev. A* **92**, 033845 (2015).
- [37] A. H. Chin, J. M. Bakker, and J. Kono, *Phys. Rev. Lett.* **85**, 3293 (2000).
- [38] L. A. Eyres, P. J. Tourreau, T. J. Pinguet, C. B. Ebert, J. S. Harris, M. M. Fejer, L. Becouarn, B. Gerard, and E. Lallier, *Appl. Phys. Lett.* **79**, 904 (2001).
- [39] O. D. Mücke, T. Tritschler, M. Wegener, U. Morgner, and F. X. Kärtner, *Phys. Rev. Lett.* **87**, 057401 (2001).
- [40] H. Hirori, K. Shinokita, M. Shirai, S. Tani, Y. Kadoya, and K. Tanaka, *Nat. Commun.* **2**, 594 (2011).
- [41] B. Zaks, H. Banks, and M. Sherwin, *Appl. Phys. Lett.* **102**, 012104 (2012).
- [42] K. Fan, H. Y. Hwang, M. Liu, A. C. Strikwerda, A. Sternbach, J. Zhang, X. Zhao, X. Zhang, K. A. Nelson, and R. D. Averitt, *Phys. Rev. Lett.* **110**, 217404 (2013).
- [43] M. S. Wismer, S. Y. Kruchinin, M. Ciappina, M. I. Stockman, and V. S. Yakovlev, *Phys. Rev. Lett.* **116**, 197401 (2016).
- [44] S. Liu, M. B. Sinclair, S. Saravi, G. A. Keeler, Y. Yang, J. Reno, G. M. Peake, F. Setzpfandt, I. Staude, T. Pertsch, and I. Brener, *Nano Lett.* **16**, 5426 (2016).
- [45] C. Schmidt, J. Btesihler, A.-C. Heinrich, J. Allerbeck, R. Podzimski, D. Berghoff, T. Meier, W. G. Schmidt, C. Reichl, W. Wegscheider, D. Brida, and A. Leitenstorfer, *Nat. Commun.* **9**, 2890 (2018).
- [46] F. Schlaepfer, M. Lucchini, S. A. Sato, M. Volkov, L. Kasmi, N. Hartmann, A. Rubio, L. Gallmann, and U. Keller, *Nat. Phys.* **14**, 560 (2018).
- [47] A. Ghalgaoui, K. Reimann, M. Woerner, T. Elsaesser, C. Flytzanis, and K. Biermann, *Phys. Rev. Lett.* **121**, 266602 (2018).
- [48] P. Xia, C. Kim, F. Lu, T. Kanai, H. Akiyama, J. Itatani, and N. Ishii, *Opt. Express* **26**, 29393 (2018).
- [49] J. Lu, E. F. Cunningham, Y. S. You, D. A. Reis, and S. Ghimire, *Nat. Photon.* **13**, 96 (2019).
- [50] J. M. Luttinger and W. Kohn, *Phys. Rev.* **97**, 869 (1955).
- [51] S. L. Chuang, *Phys. Rev. B* **43**, 9649 (1991).
- [52] D. Ahn, S. J. Yoon, S. L. Chuang, and C.-S. Chang, *J. Appl. Phys.* **78**, 2489 (1995).
- [53] P. Pfeffer and W. Zawadzki, *Phys. Rev. B* **53**, 12813 (1996).
- [54] C. Pryor, *Phys. Rev. B* **57**, 7190 (1998).
- [55] A. Dargys, *Phys. Rev. B* **66**, 165216 (2002).
- [56] S. Tomic487, A. G. Sunderland, and I. J. Bush, *J. Mater. Chem.* **16**, 1963 (2006).
- [57] A. Luque, A. Panchak, A. Mellor, A. Vlasov, A. Martí, and V. Andreev, *Sol. Energy Mater. Sol. Cells* **141**, 39 (2015).
- [58] C. M. O. Bastos, F. P. Sabino, P. E. F. Junior, T. Campos, J. L. F. D. Silva, and G. M. Sipahi, *Semicond. Sci. Technol.* **31**, 105002 (2016).
- [59] D. Sytnyk and R. Melnik, *arXiv:1808.06988*.
- [60] F. Lu, P. Xia, Y. Matsumoto, T. Kanai, N. Ishii, and J. Itatani, *Opt. Lett.* **43**, 2720 (2018).
- [61] See Supplemental Material at <http://link.aps.org/supplemental/10.1103/PhysRevB.104.L121202> for additional details of the experiment and calculation, which includes Refs. [10,18,21,29–36,48,50–60,62,64,66,68,69,79–88].
- [62] A. Zaïr, M. Holler, A. Guandalini, F. Schapper, J. Biegert, L. Gallmann, U. Keller, A. S. Wyatt, A. Monmayrant, I. A. Walmsley, E. Cormier, T. Auguste, J. P. Caumes, and P. Salières, *Phys. Rev. Lett.* **100**, 143902 (2008).
- [63] In our study, the Hamiltonian was written in the velocity gauge, where the light-matter interaction is expressed as $-A \cdot p$ by

- using the Bloch basis. On the other hand, in recent theoretical papers, the Hamiltonian is written in the length gauge, where the light-matter interaction is expressed as $-E \cdot x$ by using the Houston basis. In this alternative formulation, the electron wave number is shifted by the external field. We note that these two formulations are mathematically equivalent with each other (see Sec. III of Supplemental Material).
- [64] H. Haug and S. W. Koch, *Quantum Theory of the Optical and Electronic Properties of Semiconductors* (World Scientific, Singapore, 2009).
- [65] G. Bastard, *Wave Mechanics Applied to Semiconductor Heterostructures* (Editions de Physique, Les Ulis, France, 1988).
- [66] T. Tamaya, A. Ishikawa, T. Ogawa, and K. Tanaka, *Phys. Rev. Lett.* **116**, 016601 (2016).
- [67] E. O. Kane, *J. Phys. Chem. Solids* **1**, 249 (1957).
- [68] T. Tamaya, A. Ishikawa, T. Ogawa, and K. Tanaka, *Phys. Rev. B* **94**, 241107(R) (2016).
- [69] T. Tamaya and T. Kato, *Phys. Rev. B* **100**, 081203(R) (2019).
- [70] The band modification term $\epsilon(k_z, t)$ is ignored in conventional nonlinear optics [29–31].
- [71] For a detailed discussion, please see Sec. II in the Supplemental Material and Ref. [69].
- [72] D. H. Dunlap and V. M. Kenkre, *Phys. Rev. B* **34**, 3625 (1986).
- [73] F. Grossmann, T. Dittrich, P. Jung, and P. Hänggi, *Phys. Rev. Lett.* **67**, 516 (1991).
- [74] T. Oka, R. Arita, and H. Aoki, *Phys. B: Condens. Matter* **359**, 759 (2005).
- [75] H. Lignier, C. Sias, D. Ciampini, Y. Singh, A. Zenesini, O. Morsch, and E. Arimondo, *Phys. Rev. Lett.* **99**, 220403 (2007).
- [76] C. Gohle, T. Udem, M. Herrmann, J. Rauschenberger, R. Holzwarth, H. A. Schuessler, F. Krausz, and T. W. Hänsch, *Nature (London)* **436**, 234 (2005).
- [77] D. C. Yost, T. R. Schibli, J. Ye, J. L. Tate, J. Hostetter, M. B. Gaarde, and K. J. Schafer, *Nat. Phys.* **5**, 815 (2009).
- [78] A. Cingöz, D. C. Yost, T. K. Allison, A. Ruehl, M. E. Fermann, I. Hartl, and J. Ye, *Nature (London)* **482**, 68 (2012).
- [79] T. Tamaya and T. Kato, *Phys. Rev. B* **103**, 205202 (2021).
- [80] K. S. Virk and J. E. Sipe, *Phys. Rev. B* **76**, 035213 (2007).
- [81] I. Floss, C. Lemell, G. Wachter, V. Smejkal, S. A. Sato, X.-M. Tong, K. Yabana, and J. Burgdörfer, *Phys. Rev. A* **97**, 011401(R) (2018).
- [82] C. Q. Abadie, M. Wu, and M. B. Gaarde, *Opt. Lett.* **43**, 5339 (2018).
- [83] E. S. Toma, P. Antoine, A. de Bohan, and H. G. Müller, *J. Phys. B: At. Mol. Opt. Phys.* **32**, 5843 (1999).
- [84] G. Vampa, T. J. Hammond, M. Taucer, X. Ding, X. Ropagnol, T. Ozaki, S. Delprat, M. Chaker, N. Thiré, B. E. Schmidt, F. Légaré, D. D. Klug, A. Y. Naumov, D. M. Villeneuve, A. Staudte, and P. B. Corkum, *Nat. Photon.* **12**, 465 (2018).
- [85] A. Couairon and A. Mysyrowicz, *Phys. Rep.* **441**, 47 (2007).
- [86] W. C. Hurlbut, Y.-S. Lee, K. Vodopyanov, P. Kuo, and M. Fejer, *Opt. Lett.* **32**, 668 (2007).
- [87] M. Wegener, *Extreme Nonlinear Optics: An Introduction* (Springer Science & Business Media, New York, 2005).
- [88] J. H. Eberly, J. Javanainen, and K. Rzaczewski, *Phys. Rep.* **204**, 331 (1991).